AAS 25-866

LOCAL NORMAL FORM ANALYSIS OF HAMILTONIAN PERIODIC ORBITS UNDER FIRST-ORDER PERTURBATIONS

Andrew Langford* **and Kathleen C. Howell†**

This paper proposes an application of Hamiltonian Perturbation Theory (HPT) to analyze the persistence of periodic orbits in globally non-integrable dynamical systems under external perturbations. By leveraging the local integrability of the tangent bundle around periodic orbits, a systematic framework is developed to extend classical HPT techniques beyond their traditional domain of globally integrable systems. The approach applies Jordan Normal Form decompositions of monodromy matrices to construct canonical coordinate systems where perturbation effects can be analyzed using classical techniques. The methodology is demonstrated through detailed analysis of pitchfork bifurcations under symmetry-breaking perturbations, revealing how the canonical transformation framework predicts the emergence of cusp catastrophe structures. Application to first-order mean motion resonances in the Circular Restricted Three-Body Problem validates the theoretical predictions, showing strong qualitative agreement between the derived normal forms and numerical continuation results. This work provides a framework that can be extended to predict general orbit persistence under external disturbance applicable to mission design in sensitive dynamical environments.

1. INTRODUCTION

Cislunar mission design frequently employs long-baseline reference trajectories ($\gtrsim$ 2 years) for planning sustainable operations in dynamically sensitive regions, e.g., libration points. These reference trajectories are typically derived from periodic orbits in the Circular Restricted Three-Body Problem (CR3BP) and converged as ballistic solutions over 10^1–10^3 revolutions in cislunar ephemeris dynamical models. Constructing such ballistic trajectories in high-fidelity gravitational models, however, requires that these periodic structures persist under the unmodeled dynamical perturbations that distinguish ephemeris models from the idealized CR3BP system.

In cislunar space, gravitational perturbations to CR3BP periodic orbits are effectively represented by nonlinear, periodic terms arising from Earth-Moon pulsation and solar direct and indirect forcing.[1] Park and Howell identified the most dominant of these disturbing frequencies—specifically the Earth-Moon anomalistic and Sun–Earth-Moon sidereal frequencies—which occur at dynamical timescales ($t_{\text{dyn}} = \omega^{-1}$) of approximately 4 days when observed in high-fidelity analogs to CR3BP orbits.[2] Building on this understanding, recent studies have shown that intermediate models such as the Elliptic Restricted Three-Body Problem (ER3BP) and Hill Restricted Four-Body Problem (HR4BP) systematically capture portions of these quasi-periodic disturbances, demonstrating both frequency correspondence and geometric similarity with solutions in ephemeris models.[3–5]

*PhD Student, Hertz Fellow, NSF Graduate Research Fellow, School of Aeronautics and Astronautics, Purdue University, West Lafayette, IN 47906, langfora@purdue.edu

†Hsu Lo Distinguished Professor, School of Aeronautics and Astronautics, Purdue University, howell@purdue.edu

Multi-year ballistic baselines derived from CR3BP orbits within ephemeris-derived dynamics models experience 10^2–10^3 t_{dyn} of external disturbances beyond the CR3BP dynamics. If these disturbances introduce instability to the CR3BP orbit, constructing robust multi-year ballistic reference trajectories becomes challenging. Conversely, if disturbances do not induce instability, the resulting trajectories exist as quasi-periodically forced analogs of the original CR3BP periodic orbits, exhibiting additional frequencies attributed to each dominant forcing mechanism. Identifying and understanding sensitive transition regions arising from quasi-periodic disturbances is thus critical for robust mission trajectory design in cislunar space.

Current Methodologies and Limitations

To address the challenge of trajectory transition across model fidelity, current differential corrections methodologies include direct transition, homotopy continuation, and pseudo-arclength continuation. Each approach offers distinct advantages and diagnostic capabilities, but all share fundamental limitations in predicting orbit persistence.

The direct transition approach solves for a continuous trajectory within a given dynamical model, starting from an initial guess formed by stacking multiple revolutions of the underlying periodic orbit. When successful, continuity constraints along the discretized trajectory are maintained by local quasi-periodic structures that confine the ballistic trajectory over the desired interval. This method offers the greatest flexibility among transition strategies due to the underdetermined nature of continuity targeting, which avoids imposing strict boundary conditions. However, direct transition can fail to converge on continuous solutions over the desired baseline length without providing a robust indication of whether the failure encountered is caused by numerical or dynamical sensitivity.

Homotopy continuation employs a parameterized evolution of the dynamical system, smoothly transitioning from the original to the desired model through a series of intermediate systems, and solves identical constraints at incremental parameter values along this path. While intermediate solutions obtained during this transition may be non-physical, they can significantly improve convergence when the initial guess is distant from the desired solution. The method's effectiveness depends critically on both the chosen homotopy path and the selection of intermediate models. When homotopy continuation fails, it typically occurs at an intermediate homotopy parameter value, providing some indication of the disturbance level at which the solution breaks down and offering more diagnostic information than direct transition failures.

Pseudo-arclength continuation appends the transition parameter as an additional free variable to an initially square system—one with equal numbers of unknowns and constraints—limiting application to targeting periodic or quasi-periodic boundary conditions. This added degree of freedom produces a one-dimensional null-space of the constraint vector's Jacobian, which represents the tangent vector along the constraint manifold. Consequently, this continuation strategy can successfully navigate the smooth evolution of the solution curve, including turning points where the tangent direction becomes normal to the parameter direction. This capability allows pseudo-arclength continuation to reveal fundamental limits to particular solution existence and provide the clearest signature of transition sensitivity.

A common limitation among these methodologies is their reliance on evaluating the persistence of individual solutions, then assembling these results to construct a global picture of phase space deformation. Consequently, predictions for the existence of counterparts in perturbed models are empirically based; each disturbance case must be tested on particular orbits rather than using an

underlying predictive model to identify which orbits are susceptible to transition sensitivity from a given disturbance. This paper introduces formalisms from Hamiltonian Perturbation Theory (HPT) to develop a unifying approach for understanding how nonlinear periodic orbits deform and persist under periodic disturbances, providing both predictive capability and insight into the underlying dynamical mechanisms.

Hamiltonian Perturbation Theory

Hamiltonian Perturbation Theory (HPT) offers a framework for analyzing orbit persistence by recasting the effect of perturbations as a coordinate transformation of the original system. Rather than directly computing perturbed trajectories, the perturbation is absorbed into a near-identity canonical transformation that shifts the perturbing terms to higher order. Because the transformation is symplectic, Hamilton's equations remain valid in the new coordinates with the transformed Hamiltonian. If perturbation terms can be eliminated to the desired order, the original periodic or quasi-periodic motion persists; when resonances obstruct this elimination, the invariance of the structure may be lost and regular motion can break down.

Classical applications of HPT emphasize integrable systems subjected to small non-integrable perturbations. In this setting, algorithmic procedures such as the Lie–Deprit method construct higher-order approximations to the canonical transformation through iterative Lie transformations.[6] These techniques have proven effective when the unperturbed system admits exact analytic solutions, enabling precise characterization of how phase space structures deform and the conditions under which regular motion persists. HPT is especially well-suited for periodic disturbances, since the framework naturally represents successive orders of perturbations through Fourier expansions in characteristic frequencies. This property makes HPT an attractive approach for understanding the dominant periodic forcings identified by Gomez and Park et al. in cislunar ephemeris dynamical models.[2,7] Although cislunar models are globally non-integrable and lack closed-form solutions, large regions of phase space nevertheless host families of periodic or quasi-periodic solutions with local integrability. A local HPT treatment centered on these solutions remains both feasible and informative for predicting orbit persistence under model deformation.

Paper Approach and Contribution

This work addresses the limitations of current numerical methods by leveraging the local geometric structure that emerges around periodic orbits in globally non-integrable systems. Periodic orbits generate a natural foliation of phase space where local integrability arises, since the tangent bundle of any periodic orbit admits exactly integrable dynamics and yields a well-defined coordinate system in its neighborhood. This property enables the systematic application of classical HPT techniques without requiring global integrability. Rather than characterizing perturbations empirically across the entire phase space, their effects can instead be analyzed within these local integrable charts. Applying HPT in this setting reveals how external disturbances interact with the local dynamical structure and predicts whether the orbit can accommodate perturbations through a near-identity canonical transformation.

This approach reframes the persistence problem, shifting the focus from empirically testing individual solutions to predicting behavior directly from local geometric properties. By resolving perturbations in the neighborhood of any numerically computed periodic orbit, the method provides both existence predictions under model deformation and insight into the mechanisms that govern

orbit persistence. In this way, the framework extends classical HPT into a local setting around periodic orbits, laying the foundation for future application to astrodynamics problems while preserving the theoretical rigor and predictive power of the canonical transformation approach.

2. HAMILTONIAN SYSTEMS AND SYMPLECTIC PERTURBATION METHODS

This section develops the background needed to frame local normal forms, coordinate-free differential analysis, and perturbation methods used throughout the paper. The presentation aims to connect concepts from differential topology with Hamiltonian mechanics, two perspectives that are rarely introduced together but prove highly complementary. A modest degree of abstraction helps place Hamiltonian concepts in context and clarifies structures that might otherwise seem unmotivated or disconnected from applications. For readers seeking more comprehensive treatments, references include Goldstein,[8] Arnold,[9] and Lee,[10] with Peterson[11] providing an modern astrodynamics-oriented perspective. Readers primarily interested in applications may proceed directly to Section 5.

Symplectic Manifolds

The $2n$-dimensional phase space of a Hamiltonian system is a smooth manifold, $\mathcal{P}$, that is not intrinsically equipped with coordinates. In an abstract sense, one chooses a coordinate chart, $\psi : U \subseteq \mathcal{P} \to \mathbb{R}^{2n}$, to map domains of the manifold to a coordinate representation. This coordinate freedom is responsible for the varying dynamical evolution of the same trajectory in different sets of coordinates – for instance, a closed trajectory may appear oscillatory in Cartesian variables but reduce to uniform linear motion in another coordinate system. The compatibility between different coordinate charts is specified by the local structure of the manifold at each point, $z \in \mathcal{P}$, within their overlapping domains, $U \cap V \subseteq \mathcal{P}$. The local structure of smooth manifolds is studied via tangent spaces, $T_z\mathcal{P}$, which are vector spaces at each point z. The disjoint union of these tangent spaces and the manifold forms the tangent bundle,

$$T\mathcal{P} \;=\; \bigsqcup_{z\in\mathcal{P}} T_z\mathcal{P} \;=\; \big\{(z,v) \;\big|\; z\in\mathcal{P},\; v\in T_z\mathcal{P}\big\}.$$

Tangent vectors, $\delta z \in T_z\mathcal{P}$, capture infinitesimal displacements or variations from the reference state, z, allowing for differentiable analysis of the manifolds local behavior. An example of a tangent vector is the velocity, $\dot{z} \in T_z\mathcal{P}$, of a curve passing through the point z. Smooth maps naturally induce linear maps between tangent spaces, and when those maps are invertible they correspond to local diffeomorphisms.

While smoothness gives rise to the local vector space structure of tangent spaces, Hamiltonian phase spaces are equipped with additional structure that determines their dynamics. This structure, the symplectic 2-form, $\omega : T_z\mathcal{P} \times T_z\mathcal{P} \to \mathbb{R}$, together with the Hamiltonian function, $H : \mathcal{P} \to \mathbb{R}$, specify the Hamiltonian vector field, $X_H : \mathcal{P} \to T_z\mathcal{P}$, for any point in the phase space through the contraction, $\iota_{X_H}\,\omega = dH$. Thus, the symplectic 2-form encodes how the Hamiltonian determines the system's dynamical evolution. In coordinates, $z = (q,p)$, the symplectic form is locally prescribed by, $\omega_z = \sum_i^n dp_i \wedge dq_i$, and its matrix representation,

$$\Omega = \begin{bmatrix} 0_{n\times n} & I_{n\times n} \\ -I_{n\times n} & 0_{n\times n} \end{bmatrix},$$

yields Hamilton's equations, $\dot{z} = \Omega\nabla_z H$. A Hamiltonian system is therefore completely defined by the triple $(\mathcal{P},\omega,H)$ consisting of the smooth manifold, the symplectic form, and the Hamiltonian function.

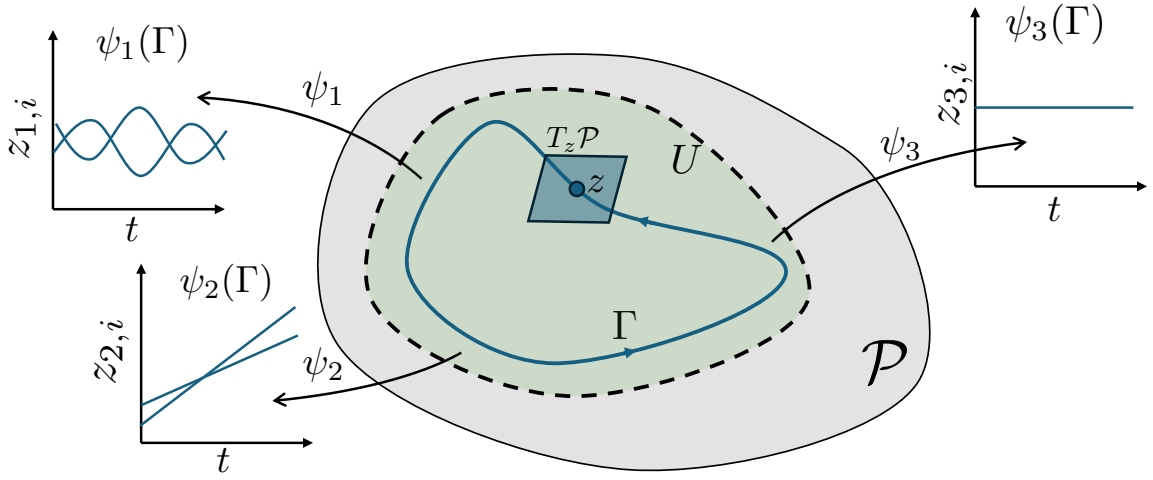

Figure 1: Phase space manifold, $\mathcal{P}$, with a periodic trajectory $\Gamma \subset \mathcal{P}$. A neighborhood $U \subset \mathcal{P}$ of Γ is covered by charts $\psi_i : U_i \to \mathbb{R}^{2n}$. At $z \in \Gamma$, the tangent space $T_z\mathcal{P}$ is shown; the tangent bundle restricted to the orbit is $T\mathcal{P}|_\Gamma = \bigsqcup_{z\in\Gamma} T_z\mathcal{P}$. The $z_{m,i}$ graphs illustrate representative $\psi_i(\Gamma)$ versus time visualizations of the same orbit.

Hamiltonian Flows and Periodic Orbit Tangent Bundle Dynamics

The Hamiltonian flow,

$$\varphi_H^t : \mathbb{R} \times \mathcal{P} \to \mathcal{P},$$

is a one-parameter mapping between points in the phase space, with the tangent vector at each point z given by the Hamiltonian vector field X_H. In practice, the flow is approximated by numerically integrating the $2n$ equations of motion given by Hamilton's equations. The state z at time t is obtained by evaluating $z = \varphi_H^t(z_0)$ for the initial condition z_0.

The differential of the flow map,

$$d\varphi_H^t : T_{z_0}\mathcal{P} \to T_z\mathcal{P},$$

maps tangent vectors $\delta z_0 \in T_{z_0}\mathcal{P}$ at z_0 to tangent vectors $\delta z \in T_z\mathcal{P}$ at $z = \varphi_H^t(z_0)$. In coordinate representation, this linear mapping is given by the State Transition Matrix (STM), $\Phi_{t_0}^t$. Hamiltonian flows preserve the symplectic form, so the differential in coordinates satisfies the *symplectic transformation condition*, $(\Phi_{t_0}^t)^\top \Omega \Phi_{t_0}^t = \Omega$. It follows that the *infinitesimal symplectic condition*, $(\dot{\Phi}_{t_0}^t)^\top \Omega + \Omega \dot{\Phi}_{t_0}^t = 0$, is satisfied for the generator of the flow differential, $\dot{\Phi}_{t_0}^t = \Omega \nabla^2 H \Phi_{t_0}^t$.

This investigation leverages the natural structure that exists around T-periodic Hamiltonian flows, $\varphi_H^T z = z \; \forall \; z \in \Gamma \subset \mathcal{P}$. The tangent bundle restricted to the periodic orbit,

$$T\mathcal{P}|_\Gamma = T\Gamma \oplus N\Gamma,$$

is composed of the tangent bundle restricted to the 1D curve, $T\Gamma = \{(z, v) \in T\mathcal{P} \;\big|\; z \in \Gamma,\; T_z\Gamma = \text{Span}\{X_H(z)\}\}$, and its transverse bundle, $N\Gamma = \{(z, v) \in T\mathcal{P} \;\big|\; z \in \Gamma,\; v \perp T_z\Gamma\}$. A remarkable feature is that the dynamics of $T\mathcal{P}|_\Gamma$, admit exact analytic representation through Floquet theory.[12,13] Since the dynamics of $T_z\mathcal{P}|_\Gamma$, governed by

$$\frac{d}{dt}\delta z = \Omega \nabla^2 H(\varphi_H^t(z_0))\delta z,$$

is a T-periodic linear system, Floquet theory provides the fundamental solution matrix decomposition

$$\Phi_{t_0}^{t} = P(t)e^{S(t-t_0)}P^{-1}(t_0),$$

where $P(t)$ is a T-periodic matrix of Floquet modal vectors and $e^{S(t-t_0)}$ is block diagonal and encodes the linear modal structure of the tangent dynamics. Evaluating after one period, $t = t_0 + T$, shows that the eigenvalues λ_i of the monodromy matrix M coincide with the diagonal entries of e^{ST},

$$M = \Phi(t_0 + T, t_0) = P(t_0)e^{ST}P(t_0)^{-1}, \quad J := e^{ST},$$

and classically appear in reciprocal pairs $(\lambda_i, 1/\lambda_i)$ due to the symplectic nature of any Hamiltonian flow differential. Note, J, is not necessarily a diagonal matrix, due to the appearance of generalized eigenvector chains when M is defective. Williams, Langford, and Howell[14] elaborate on the origin of generalized eigenvector chains and their numerical computation for Jordan Normal Form representations of the monodromy matrix in astrodynamics applications.

Transforming variational states into modal coordinates, $\alpha = P(t)^{-1}\delta z$, yields a linear time-invariant system for the tangent dynamics

$$\frac{d}{dt}\alpha = S\alpha$$

where, $S = 1/T\log(J)$, is a $2n \times 2n$ matrix with constant coefficients.[14] If S satisfies the infinitesimal symplectic condition defined above, then the constant, S, is the generator of a local linear Hamiltonian flow on the tangent bundle, $T\mathcal{P}|_\Gamma$. The local Hamiltonian can be written in quadratic form as,

$$H(\alpha) = -\frac{1}{2}\alpha^\top \Omega S \alpha$$

and the corresponding tangent bundle vector field is given by Hamilton's equations, $\dot{\alpha} = \nabla_\alpha \Omega H$. This local quadratic Hamiltonian represents a *locally integrable system of infinitesimal deviations* around the periodic orbit. Although finite deviations from the orbit do not follow these exact linearized dynamics, the local frame is well suited to capture the effects of infinitesimal perturbations. This feature provides a foundation for the systematic application of HPT methodologies to globally non-integrable systems admitting periodic motion.

Local Integrals of the Motion and Canonical Coordinates

The integrability of the tangent bundle dynamics around a periodic orbit provides a natural framework for introducing dynamically motivated coordinate bases in the surrounding phase space. Consider a smooth function $f : \mathcal{P} \to \mathbb{R}$ evolving along the Hamiltonian flow φ_H^t. Its time derivative is

$$\dot{f} \;=\; \sum_{i=1}^{n}\Big(\frac{\partial f}{\partial q_i}\dot{q}_i + \frac{\partial f}{\partial p_i}\dot{p}_i\Big) \;=\; \sum_{i=1}^{n}\Big(\frac{\partial f}{\partial q_i}\frac{\partial H}{\partial p_i} - \frac{\partial f}{\partial p_i}\frac{\partial H}{\partial q_i}\Big) \;=\; \{f, H\},$$

where $\{f, H\}$ is the Poisson bracket of f with the Hamiltonian H. The Poisson bracket defines the Lie derivative

$$\mathcal{L}_H : C^\infty(\mathcal{P}) \to C^\infty(\mathcal{P}),$$

which measures how functions evolve along the Hamiltonian flow. A few simple examples include $\mathcal{L}_H p_i = \{p_i, H\} = -\partial H/\partial q_i$, $\mathcal{L}_H q_i = \{q_i, H\} = \partial H/\partial p_i$, and $\mathcal{L}_H H = \{H, H\} = 0$ for time-autonomous systems. A function $I : \mathcal{P} \to \mathbb{R}$ is an integral of the motion if $\{I, H\} = 0$. A

Hamiltonian system is Liouville integrable if its $2n$-dimensional phase space admits n functionally independent integrals that mutually commute, $\{I_i, I_j\} = 0$ for all i, j. The Liouville–Arnold theorem then guarantees the existence of canonical action–angle coordinates (I_i, ϕ_i) with $\{I_i, H\} = 0$ and $\{\phi_i, H\} = c \in \mathbb{R}$.[9]

Local integrability around periodic orbits is revealed through conserved quantities of the linearized dynamics, identifiable from the eigenstructure of the monodromy matrix. Suppose $I : \mathcal{P} \to \mathbb{R}$ is conserved along a T-periodic orbit so that $I(\varphi_H^t(z_0)) = I(z_0)$. Differentiating gives

$$\nabla I(\varphi_H^t z_0)\Phi_{t_0}^t = \nabla I(z_0),$$

linking the gradient of I to the STM. Evaluating after one period, $t = T + t_0$ with $\varphi_H^T(z_0) = z_0$, shows that ∇I is a left eigenvector of the monodromy matrix M with unit eigenvalue, $\nabla I(z_0)M = \nabla I(z_0)$. For a symplectic matrix M, if $Mv = \lambda v$ then $w^\top = -v^\top\Omega$ is a left eigenvector with eigenvalue $1/\lambda$. Hence, each conserved quantity I corresponds to a Hamiltonian vector field $X_I = \Omega\nabla I$ that is a right eigenvector of M with eigenvalue one. In particular, since H is conserved, $X_H = \Omega\nabla H$ is always such an eigenvector.

In autonomous Hamiltonian systems, periodic orbits always produce a unit eigenvalue with algebraic multiplicity two but geometric multiplicity one, yielding a generalized eigenvector chain of length two.[14] The first eigenvector $v_\phi = X_H(z_0)$ corresponds to the phase (time-shift) direction along the orbit. The second unit direction arises as a generalized eigenvector v_I satisfying $(M - I)v_I = Tv_\phi$, obtained by differentiating the periodic orbit with respect to a parameter that shifts energy or period. Together, (v_ϕ, v_I) span the $\lambda = 1$ Jordan block and define a canonical basis pair $(\hat{\phi}_\Gamma, \hat{I}_\Gamma)$ in the tangent space, where $\hat{\phi}_\Gamma$ points along the orbit and $\hat{I}_\Gamma$ is its conjugate. Symplectic normalization enforces $\hat{I}_\Gamma^\top\Omega\hat{\phi}_\Gamma = 1$, achieved by scaling with $v_I^\top\Omega v_\phi = s$ and setting $\hat{\phi}_\Gamma := v_\phi$, $\hat{I}_\Gamma := v_I/s$.

For non-bifurcating orbits, the remaining eigenvalues typically occur as real pairs $\lambda_{1,2} = e^{\pm aT}$ or complex conjugates on the unit circle $\lambda_{1,2} = e^{\pm i\omega T}$. Their eigenvectors span the hyperbolic and center subspaces, providing canonical basis pairs for those dynamics. Hyperbolic eigenvectors align with stable and unstable manifolds and, after symplectic normalization, define the basis $(\hat{q}_h, \hat{p}_h)$ with $\hat{q}_h^\top\Omega\hat{p}_h = 1$. Normalization can be achieved by evaluating $v_1^\top\Omega v_2 = s$ and setting $\hat{q}_h = s^{-1/2}v_1$, $\hat{p}_h = s^{-1/2}v_2$. Complex center eigenvectors are not unique, but realifying v_c as $v_1 = \mathrm{Re}(v_c)$ and $v_2 = -\mathrm{Im}(v_c)$ yields a unique real basis for the center subspace. Although v_1 and v_2 are no longer eigenvectors of M, they span the eigenspace E_c and can be symplectically normalized to define the canonical basis $(\hat{q}_c, \hat{p}_c)$ with $\hat{q}_c^\top\Omega\hat{p}_c = 1$.

By symplectically normalizing the eigendirections of the monodromy matrix, one obtains canonical basis pairs in the tangent space for the longitudinal, hyperbolic, and center dynamics. Variational states are then expressed by projecting onto the associated dual covectors, i.e., the rows of the inverse modal map. This produces the local canonical coordinate system

$$\delta z = (\phi_\Gamma, I_\Gamma, q_c, p_c, q_h, p_h),$$

where (ϕ_Γ, I_Γ) represent the phase–action pair along the orbit, and (q_c, p_c), (q_h, p_h) are canonical coordinates in the center and hyperbolic subspaces. In quadratic Hamiltonian form,[14] the quantities I_Γ, $I_c = \frac{1}{2}(q_c^2 + p_c^2)$, and $I_h = q_h p_h$ emerge as canonical invariants. These invariants render the dynamics separable and integrable on the periodic orbit's tangent bundle.

By symplectically normalizing the eigendirections of the monodromy matrix, one obtains canonical basis pairs in the tangent space for the longitudinal, hyperbolic, and center dynamics. Variational states are then expressed by projecting onto the associated dual covectors, i.e., the rows of the inverse modal map. This produces the local canonical coordinate system

$$\delta z = (\phi_\Gamma, I_\Gamma, q_c, p_c, q_h, p_h),$$

where (ϕ_Γ, I_Γ) represent the phase–action pair along the orbit, and (q_c, p_c), (q_h, p_h) are canonical coordinates in the center and hyperbolic subspaces. In quadratic Hamiltonian form,[14] the quantities I_Γ, $I_c = \frac{1}{2}(q_c^2 + p_c^2)$, and $I_h = q_h p_h$ emerge as canonical invariants. These invariants render the dynamics separable and integrable on the periodic orbit's tangent bundle. Among them, the longitudinal action requires special interpretation. The physical action of the periodic family is the non-negative quantity $\mathcal{I}(\Gamma) = (2\pi)^{-1} \oint_\Gamma p \cdot dq$. In the local normal form it is more natural to expand in a signed detuning variable

$$I_\Gamma := \mathcal{I}(\Gamma) - \mathcal{I}(\Gamma_0),$$

defined relative to a chosen base orbit Γ_0 with $\mathcal{I}(\Gamma_0) > 0$. This convention preserves the canonical structure and makes clear that I_Γ in the linearization measures detuning, while the physical action remains $\mathcal{I}(\Gamma) \geq 0$. In this sense, the projection of a variational state onto the longitudinal basis vector $\hat{I}_\Gamma$ recovers the signed detuning coordinate.

3. PERIODIC ORBIT NORMAL FORMS

The tangent bundle restricted to a periodic orbit, $T\mathcal{P}|_\Gamma$, admits locally integrable dynamics through the eigenstructure of the monodromy matrix. As established in the previous section, symplectic normalization of the monodromy eigenvectors provides canonical coordinates in which the linearized flow becomes separable and Hamiltonian. This section examines how different Jordan block structures of the monodromy matrix give rise to distinct local normal forms, each encoding specific bifurcation behaviors and dynamical transitions.

The Jordan Normal Form decomposition of the monodromy matrix, M, yields block diagonal structure $J = e^{ST}$ where each 2×2 block corresponds to a particular type of local dynamics. The 2×2 block matrices that appear in CR3BP JNF decompositions of the monodromy matrix can be classified into

longitudinal / phase–energy

$$\tilde{J}_\Gamma = \begin{pmatrix} 1 & \kappa T \\ 0 & 1 \end{pmatrix}$$

period–doubling

$$\tilde{J}_{P2} = -\begin{pmatrix} 1 & \frac{\sigma T}{2} \\ 0 & 1 \end{pmatrix}$$

pitchfork

$$\tilde{J}_\psi = \begin{pmatrix} 1 & \sigma T \\ 0 & 1 \end{pmatrix}$$

centre n–period

$$\tilde{J}_{Pn} = \mathrm{diag}\big(e^{i2\pi/n},\, e^{-i2\pi/n}\big)$$

hyperbolic

$$\tilde{J}_\mathcal{N} = \mathrm{diag}\big(\lambda,\, \lambda^{-1}\big)$$

In the doubled stroboscopic map (period $2T$), the period–doubling block becomes the pitchfork block $(J_{P2})^2 = J_\psi$. Thus, a -1 multiplier with a length-2 Jordan chain at period T is equivalent, in the $2T$-map, to a $+1$ multiplier with the same Jordan structure. The two cases therefore share the same local normal form once the time base is doubled; only the interpretation differs. Each block type generates a specific local Hamiltonian structure through a systematic construction process: (i) bringing J to its symplectic Jordan form, (ii) choosing a symplectically normalized modal basis P such that $P^T \Omega P = \Omega$, and (iii) transforming to modal coordinates $\alpha = P^{-1}\delta z$. In this

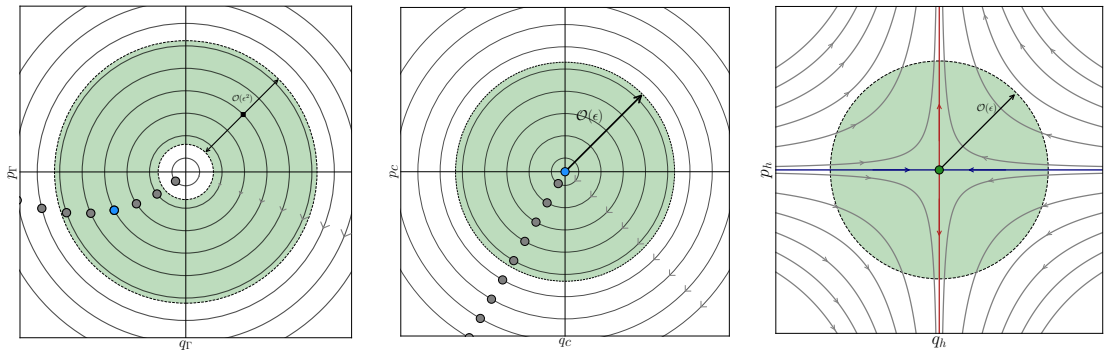

Figure 2: Phase space representation of a local normal form about a non-bifurcating orbit with a center-hyperbolic transverse subspace.

canonical basis, the constant matrix $S = \frac{1}{T}\log(J)$ becomes block diagonal and, when it satisfies the infinitesimal symplectic condition $S^T\Omega + \Omega S = 0$, the modal coordinate dynamics $\dot{\alpha} = S\alpha$ can be expressed through Hamilton's equations with a quadratic Hamiltonian $H^{(2)} = \frac{1}{2}\alpha^T K \alpha$ where $S = \Omega K$. A detailed derivation of this monodromy matrix to local Hamiltonian is presented in Williams, Langford, and Howell.[14] The remaining text in this section will discuss the local Hamiltonian's associated with non-bifurcating, period multiplying, cyclic-fold, and pitchfork bifurcations.

Non-bifurcating Orbit Normal Forms

For a non-bifurcating periodic orbit with transverse subspace decomposed as $\mathcal{N} = E_c \oplus E_h$, the local canonical coordinates $(\phi_\Gamma, I_\Gamma, q_c, p_c, q_h, p_h)$ provide a separable Hamiltonian,

$$H = \omega_\Gamma I_\Gamma + \frac{1}{2}\kappa I_\Gamma^2 + \omega_c I_c + \gamma I_h$$

where the canonical actions are $I_c = \frac{1}{2}(q_c^2 + p_c^2)$ and $I_h = q_h p_h$, and the coefficients $\omega_\Gamma = T/2\pi$, $\omega_c = \arg(\lambda)/T$, and $\gamma = |\log(\lambda)|$ are computed from the period and eigenvalues of the monodromy matrix. This normal form reveals several key features of the local dynamics. For one, the longitudinal subspace includes the quadratic term I_Γ^2, which yields a non-degenerate frequency $\dot{\phi}_\Gamma = \omega_\Gamma + \kappa I_\Gamma$, capturing the phase drift (non-isochrony) observed in families of nearby periodic orbits. Meanwhile, the center subspace exhibits constant frequency $\dot{\phi}_c = \omega_c$ at quadratic order, requiring higher-order terms to capture amplitude-dependent frequency variations. Phase portraits of each separable subsystem are shown for a non-bifurcating orbit in Figure 2. The complete integrability of this local system—with three conserved actions I_Γ, I_c, and I_h—provides the foundation for perturbation analysis. External disturbances can be systematically analyzed in these coordinates to determine whether the canonical transformation can accommodate the perturbation while preserving the essential dynamical structure.

Period–Multiplying Orbit and Resonant Normal Forms

At a period–multiplying bifurcation, $J = \mathrm{diag}(\tilde{J}_\Gamma, \tilde{J}_{Pn})$, the longitudinal and center frequencies satisfy a near–integer resonance $\omega_\Gamma \approx n\,\omega_c$, with $n \in \mathbb{Z} \setminus \{0\}$. This motivates introducing the detuning variable $\delta := \omega_\Gamma - n\,\omega_c \ll 1$. The quadratic Hamiltonian derived from the symplectically

normalized Jordan blocks is

$$H(I_\Gamma, I_c) = \omega_\Gamma I_\Gamma + \tfrac{\kappa}{2} I_\Gamma^2 + \omega_c I_c, \qquad I_c = \tfrac{1}{2}(q_c^2 + p_c^2).$$

Because H depends only linearly on I_c at quadratic order, it misleadingly suggests a continuous family of period–n orbits filling the (q_c, p_c) plane. In the nonlinear system, only a discrete set of branches appears,[15] revealing the necessity of resonant terms beyond quadratic order.

The standard resonant–averaging procedure clarifies which terms survive. Monomials of the form $I_\Gamma^m I_c^k e^{i(m\phi_\Gamma + k\phi_c)}$ average to zero unless $m\omega_\Gamma + k\omega_c = 0$. At an n:1 internal resonance, the combination $(m, k) = (-1, n)$ satisfies this condition, leaving a harmonic $\cos(n\phi_c - \phi_\Gamma)$ as the first nonvanishing angle–dependent term.[13] Introducing the slow resonant angle $\Psi = n\phi_c - \phi_\Gamma$ and the center amplitude $\Sigma = \sqrt{2I_c}$, the resonant normal form becomes

$$H_{\text{res}}(I_\Gamma, \Sigma, \Psi) = \delta\, I_\Gamma + \tfrac{\kappa}{2} I_\Gamma^2 + \tfrac{\alpha}{2} I_\Gamma \Sigma^2 + \tfrac{\beta}{4}\Sigma^4 + A_n\, \Sigma^n \cos\Psi,$$

where α, β are normal–form coefficients and A_n is the leading resonant coupling constant. The quartic terms represent the lowest nonlinear corrections in the Birkhoff expansion, while $\Sigma^n \cos\Psi$ is the first angle–dependent contribution permitted by the resonance condition. Equilibria of this reduced system are determined by

$$\partial_\Psi H_{\text{res}} = -A_n \Sigma^n \sin\Psi = 0 \quad \Rightarrow \quad \Psi^* \in \{0, \pi\},$$

$$\partial_\Sigma H_{\text{res}} = \alpha I_\Gamma \Sigma + \beta\Sigma^3 + n A_n \Sigma^{n-1}\cos\Psi = 0, \qquad \partial_{I_\Gamma} H_{\text{res}} = \delta + \kappa I_\Gamma + \tfrac{\alpha}{2}\Sigma^2 = 0,$$

and correspond to periodic orbits in the transverse center subspace (q_c, p_c). From the last condition, $I_\Gamma = -\frac{\delta}{\kappa} - \frac{\alpha}{2\kappa}\Sigma^2$, which, when substituted into the second relation, yields a single amplitude equation for Σ given $(\delta, \alpha, \beta, A_n)$. Factoring Σ gives

$$\Sigma\Big(\alpha I_\Gamma + \beta\Sigma^2 \pm n A_n \Sigma^{n-2}\Big) = 0,$$

with '$+$' for $\Psi^* = 0$ and '$-$' for $\Psi^* = \pi$. The trivial solution $\Sigma = 0$ corresponds to the parent orbit, while nontrivial positive real roots represent pairs of symmetric period–n branches differing by a π phase shift in Ψ.

The resonant normal form resolves the contradiction between the quadratic model's prediction of a continuum of period–n candidates and the discrete A/B branches observed numerically. Resonant coupling terms, absent at quadratic order, provide the phase–selection mechanism that collapses the continuum to discrete solutions. This framework offers a foundation for future work on using resonant normal forms about periodic orbits to study nonlinear and perturbative behavior.

Fold Bifurcations and Non-canonical Charts

Fold bifurcations pose a special challenge within the local normal form framework because their Jordan block structure breaks the symplectic normalization procedure that works for other bifurcation types. A cyclic fold in the CR3BP produces a 4×4 Jordan chain with unit eigenvalue, leading to the constant dynamics matrix

$$S = \tfrac{1}{T}\log J_{\text{fold}} = \tfrac{1}{T}\begin{bmatrix} 0 & 1 & -\frac{1}{2} & \frac{1}{3} \\ 0 & 0 & 1 & -\frac{1}{2} \\ 0 & 0 & 0 & 1 \\ 0 & 0 & 0 & 0 \end{bmatrix},$$

which governs the evolution of the modal coordinates through $\dot{\alpha} = S\alpha$. The difficulty becomes clear when testing the infinitesimal symplectic condition. Direct calculation shows that S does not satisfy $S^T\Omega + \Omega S = 0$, confirming that the raw modal coordinates $\alpha = (\alpha_1, \alpha_2, \alpha_3, \alpha_4)$ are not canonical. In particular, the pairing structure required for symplectic coordinates is absent from the cyclic–fold Jordan basis.

This failure manifests in the coupled, polynomial evolution of the modal coordinates rather than the separable dynamics seen in previous cases. For example, the explicit solution for $\alpha_1(t)$ is

$$\alpha_1(t) = \alpha_{1,0} + \alpha_{2,0}t + \tfrac{1}{2}(t^2 - t)\alpha_{3,0} + \tfrac{1}{6}(2t - 3t^2 + t^3)\alpha_{4,0},$$

showing that each component depends on multiple initial conditions through polynomial time dependence. Importantly, this coupling does not mean that the dynamics on $T\mathcal{P}|_\Gamma$ are non-Hamiltonian. Instead, constructing canonical coordinates at a fold requires an additional linear transformation beyond the direct Jordan normalization. The existence of such a symplectic transformation is guaranteed by the Hamiltonian structure of the ambient phase space, though its explicit form requires further steps than the Jordan decomposition approach outline by Williams, Langford, and Howell. Determining how to systematically construct these transformations—and whether the non-symplectic nature of the Floquet basis at cyclic folds has deeper implications for perturbation analysis—remains an important direction for future study.

Pitchfork and Period-Doubling Bifurcation Normal Forms

Pitchfork and period–doubling bifurcations share the same local structure once the latter is viewed in the doubled–period return map. In both cases the monodromy matrix contains two length–2 Jordan chains with unit multiplier,

$$J_\psi = \mathrm{diag}(\tilde{J}_\Gamma, \tilde{J}_\psi), \qquad \tilde{J}_\Gamma = \begin{pmatrix} 1 & \kappa T \\ 0 & 1 \end{pmatrix}, \qquad \tilde{J}_\psi = (\tilde{J}_{P2})^2 = \begin{pmatrix} 1 & \sigma T \\ 0 & 1 \end{pmatrix},$$

so that

$$S_\psi = \tfrac{1}{T}\log J_\psi = \mathrm{diag}\left(\begin{bmatrix} 0 & \kappa \\ 0 & 0 \end{bmatrix}, \begin{bmatrix} 0 & \sigma \\ 0 & 0 \end{bmatrix} \right).$$

After symplectic normalization, canonical pairs appear as (ϕ_Γ, I_Γ) in the longitudinal subspace and (q_c, p_c) in the center subspace. The quadratic Hamiltonian takes the form

$$H(I_\Gamma, I_c) = \omega_\Gamma I_\Gamma + \tfrac{\kappa}{2} I_\Gamma^2 + \tfrac{\sigma}{2} p_c^2, \qquad I_c = \tfrac{1}{2}(q_c^2 + p_c^2).$$

Because H is independent of q_c, the conjugate momentum p_c is conserved and the center direction appears neutrally stable. At quadratic order this yields a one–parameter continuum of equilibria in (q_c, p_c), a degeneracy reflecting that the monodromy encodes only lowest–order information near a 1:1 internal resonance. To organize higher–order terms, the expansion is centered at $I_\Gamma = 0$, corresponding to the resonant orbit around which bifurcation occurs.

Recall in a Birkhoff expansion, monomials $I_\Gamma^m I_c^k e^{i(m\phi_\Gamma + n\phi_c)}$ average away unless $m\omega_\Gamma + n\omega_c = 0$. At 1:1 resonance this condition reduces to $m + n = 0$, leaving precisely those terms depending on the slow angle $\Psi = \phi_c - \phi_\Gamma$.[13] Symmetry, however, forbids odd powers of the center amplitude $\Sigma = \sqrt{2I_c}$, and at quartic order the resonant $\cos\Psi$ contributions can be absorbed by a constant

rotation in (q_c, p_c). The result is an *action–only* averaged normal form, standard for low–order resonances, which captures the amplitude couplings without explicit angle dependence:

$$\bar{H}(I_\Gamma, I_c) = \omega_\Gamma I_\Gamma + \tfrac{\kappa}{2} I_\Gamma^2 + \sigma I_c + \alpha I_\Gamma I_c + \beta I_c^2,$$

with real coefficients α, β. Since ϕ_c is cyclic, equilibria satisfy

$$\frac{\partial \bar{H}}{\partial I_c} = \sigma + \alpha I_\Gamma + 2\beta I_c = 0 \quad \Rightarrow \quad I_c^*(I_\Gamma) = -\frac{\sigma + \alpha I_\Gamma}{2\beta}.$$

Defining $\Sigma = \mathrm{sgn}(q_c)\sqrt{2I_c}$ gives

$$\Sigma_\pm(I_\Gamma) = \pm\sqrt{-\tfrac{\sigma+\alpha I_\Gamma}{\beta}}.$$

For $I_\Gamma < I_{\mathrm{crit}} = -\sigma/\alpha$ only the central branch $\Sigma = 0$ exists, while for $I_\Gamma > I_{\mathrm{crit}}$ two symmetric branches $\Sigma_\pm$ bifurcate. A canonical shift $\tilde{I}_\Gamma = I_\Gamma + \sigma/\alpha$ recenters the bifurcation at $\tilde{I}_\Gamma = 0$, yielding the characteristic square–root scaling $\Sigma \propto \sqrt{\tilde{I}_\Gamma}$. Thus the quartic resonant normal form resolves the degeneracy of the quadratic model. The 1:1 resonance enforces a phase relation between longitudinal and center dynamics, with the pitchfork or period–doubling bifurcation generating discrete symmetric branches from the neutral center direction.

4. FIRST-ORDER PERTURBATIONS TO PITCHFORK BIFURCATIONS

The qualitative descriptions of local dynamics developed in the previous section provide a basis for modeling how external perturbations influence periodic orbits near internal resonances. Among these, pitchfork and period–doubling bifurcations are especially important because they represent the strongest form of resonance between longitudinal and center directions. Although the quadratic approximation derived from the Jordan decomposition was insufficient and required extension to higher–order resonant normal forms, this limitation does not affect its usefulness for qualitative analysis. With this local structure established, perturbation theory can now be applied to predict how small disturbances deform the surrounding phase space and modify the bifurcation structure.

Canonical Perturbation Framework

Consider a Hamiltonian system that can be written as an integrable base plus a small perturbation

$$H = H_0(I) + \epsilon H_1(I, \phi) + O(\epsilon^2)$$

where $H_0(I)$ depends only on action variables and $\epsilon \ll 1$ parameterizes the perturbation strength. The goal is to construct a near-identity canonical transformation $(I, \theta) \mapsto (I', \phi')$ through solving for its generating function, W_1, through the Lie-Deprit procedure

$$(I', \phi') = \exp(\epsilon \mathcal{L}_{W_1})(I, \phi)$$

where $\mathcal{L}_{W_1}(\cdot) = \{\cdot, W_1\}$ is the Lie derivative over the flow generated by W_1. The transformed Hamiltonian becomes

$$K = \exp(\epsilon L_{W_1}) H = H_0 + \epsilon(H_1 + \{H_0, W_1\}) + O(\epsilon^2)$$

The key insight is that the generator W_1 can be chosen to eliminate angle-dependent terms in H_1 provided they satisfy appropriate non-resonance conditions. Specifically, expanding H_1 in Fourier series $H_1 = \langle H_1 \rangle + H_{1,\text{osc}}$ where $\langle H_1 \rangle$ is the angle average, the homological equation

$$\{H_0, W_1\} + H_{1,\text{osc}} = 0$$

can be solved as $W_{1,k} = -H_{1,k}/(ik\cdot\omega)$ for each Fourier mode k, provided the denominator $k\cdot\omega \neq 0$ where $\omega = \partial H_0/\partial I$. Terms with $k \cdot \omega = 0$ represent resonances that cannot be eliminated and must be retained in the normal form.

Imperfect Pitchfork Normal Form

For the symmetric pitchfork the averaged Hamiltonian takes the form

$$\bar{H}_0(\tilde{I}_\Gamma, I_c) = \tfrac{\kappa}{2}\tilde{I}_\Gamma^2 + \alpha\tilde{I}_\Gamma I_c + \beta I_c^2$$

after shifting the longitudinal action so that the bifurcation occurs at $\tilde{I}_\Gamma = 0$. Adding a small perturbation gives

$$H = \bar{H}_0 + \epsilon H_1(\tilde{I}_\Gamma, I_c, \phi_\Gamma, \phi_c).$$

Because the longitudinal and center frequencies satisfy a 1:1 resonance, contributions depending only on the slow difference angle $\Psi = \phi_c - \phi_\Gamma$ cannot be eliminated. Writing

$$H_1 = \langle H_1 \rangle_{\text{res}} + H_{1,\text{nr}}, \qquad \langle H_1 \rangle_{\text{res}} = \sum_m H_{1,(m,-m)}(I) e^{im\Psi},$$

the generator W_1 removes the nonresonant part, leaving $K = \bar{H}_0(\tilde{I}_\Gamma, I_c) + \epsilon\langle H_1 \rangle_{\text{res}}(\tilde{I}_\Gamma, I_c, \Psi) + O(\epsilon^2)$. In the symmetric case the reduced Hamiltonian is even in the signed center amplitude $\Sigma = \sqrt{2I_c}$ and contains only even harmonics of Ψ, which reflects the discrete reflection symmetry of the center variables. A symmetry breaking perturbation removes that selection rule. The first resonant contribution that becomes admissible is linear in Σ and carries the slow angle,

$$\langle H_1 \rangle_{\text{res}} = \pi\,\Sigma\cos\Psi + O(\Sigma^3),$$

where π measures the strength of the symmetry breaking. The imperfect normal form is

$$K(\tilde{I}_\Gamma, \Sigma, \Psi) = \tfrac{\kappa}{2}\tilde{I}_\Gamma^2 + \tfrac{\alpha}{2}\tilde{I}_\Gamma\Sigma^2 + \tfrac{\beta}{4}\Sigma^4 + \epsilon\pi\Sigma\cos\Psi + O(\epsilon\Sigma^3).$$

The linear term is odd in Σ and therefore breaks the symmetric branches and captures the qualitative effect of a symmetry–breaking perturbation at 1:1 resonance.

Connection to the Second Fundamental Model of Resonance

After averaging out the fast longitudinal angle, the reduced system is effectively one degree of freedom in (Ψ, I_c). This reduction matches the Second Fundamental Model of Resonance.[16,17] By scaling time and the transverse action, the three coefficients (α, β, π) collapse to a single detuning parameter and the system is brought into the universal form

$$H_{SFMR}(x, y) = -\tfrac{1}{2}(\delta + 1)(x^2 + y^2) + \tfrac{1}{8}(x^2 + y^2)^2 - 2x$$

with $(x, y) = (\rho\cos\Psi, \rho\sin\Psi)$ and $\rho \propto \Sigma$. Pitchfork and period-doubling bifurcations under symmetry breaking perturbations are therefore locally equivalent to H_{SFMR}, whose phase portrait captures the mechanisms of resonance in the reduced center subsapce.

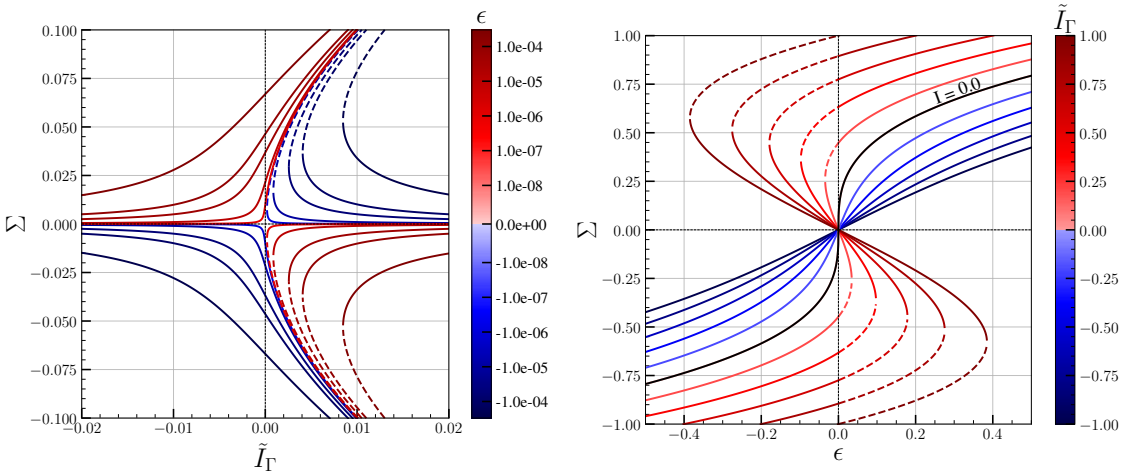

Figure 3: Both: Solutions of Equation (1) indicating the conditions for a stable (solid) and unstable (dashed) periodic solutions in the vicinity of a pitchfork bifurcation, ($\tilde{I}_\Gamma = \Sigma = 0$), under a symmetry breaking perturbation. The coefficients of the cubic solutions shown are $\alpha = \beta = 1, \pi = -1$. **Left:** Solution to Equation (1) for a range of fixed ϵ values. **Right:** Solution to Equation (1) for a range of fixed $\tilde{I}_\Gamma$ values.

Local Periodic Orbit Solutions under Perturbation

Equilibria of this perturbed system satisfy the stationary conditions

$$\frac{\partial K}{\partial \Psi} = -\epsilon\pi\Sigma \sin\Psi = 0 \quad \Rightarrow \quad \Psi^* \in \{0, \pi\}$$
$$\frac{\partial K}{\partial \Sigma} = \alpha\tilde{I}_\Gamma\Sigma + \beta\Sigma^3 + \epsilon\pi\cos\Psi^* = 0$$

Fixing the phase orientation by choosing $\cos\Psi^* = +1$, since the case $\cos\Psi^* = -1$ just corresponds to $\epsilon \mapsto -\epsilon$, the equilibrium condition reduces to the cubic,

$$\beta\Sigma^3 + \alpha\tilde{I}_\Gamma\Sigma + \pi\epsilon = 0 \tag{1}$$

K captures the local behavior of a pitchfork bifurcation under a first-order symmetry breaking perturbation. The roots of the cubic equation $\Sigma(\tilde{I}_\Gamma, \epsilon) = 0$ correspond to admissible periodic solutions under flow of the perturbed local Hamiltonian, K. Setting $\epsilon = 0$ recovers the symmetric pitchfork $\Sigma(\beta\Sigma^2 + \alpha\tilde{I}_\Gamma) = 0$, while any $\epsilon \neq 0$ unfolds this into the standard cusp catastrophe geometry.[18]

Figure 3 plots the solutions of Equation (1) to illustrate the folding and imperfect pitchfork cross sections that are characteristic of cusp catastrophe scenarios.[18] At $\epsilon = 0$, the symmetric pitchfork bifurcation appears in the $\Sigma(\tilde{I}_\Gamma)$ cross section as two branches emerging from the origin. As $|\epsilon|$ increases, the pitchfork structure deforms, creating two unconnected branches that evolve smoothly from the original parent branch $\Sigma = 0, \tilde{I}_\Gamma \neq 0$. This deformation suggests that numerical continuation procedures using pseudo-arclength methods would encounter these branches as distinct solution families rather than as a connected bifurcating structure.

The right panel of Figure 3 reveals the fundamental change in solution topology for fixed longitudinal action values. For $\tilde{I}_\Gamma > 0$, a critical value of $|\epsilon|$ exists beyond which only one real solution

remains—two periodic solutions collide and disappear while a third persists. This collision occurs at the fold points of the cusp surface, representing saddle-node bifurcations in the perturbed system. For the coefficient selection shown ($\alpha = \beta = 1, \pi = -1$), the $\Sigma < 0$ branch exists for all $\epsilon > 0$, while the $\Sigma > 0$ branch exists for all $\epsilon < 0$, demonstrating the asymmetric response to positive and negative perturbations.

The cusp structure provides a complete local description of how symmetry-breaking perturbations transform the local phase space of periodic orbits. Rather than the simultaneous destruction of branches at a critical parameter value, the perturbed system exhibits a smooth transition through the $\Sigma(\tilde{I}_\Gamma, \epsilon)$ space, with hysteresis effects and a sudden breakdown of periodic orbits only occurring at $|\epsilon| > 0$ values. This behavior is fundamental to understanding how periodic orbit families respond to external forcing and how the continuation into periodically perturbed systems may disrupt periodic orbit structure.

The construction of this local normal form methodology around periodic orbits enables direct application of Lie-Deprit perturbation theory to locally integrable regions of a non-integrable phase space. This approach provides a systematic framework for predicting how specific types of perturbations will modify the structure of periodic orbit families. The methodology bridges the gap between classical dynamical systems theory and numerical computation of nonlinear periodic orbits, offering both qualitative insight into bifurcation mechanisms and quantitative predictions that can be directly tested against numerical continuation results.

5. APPLICATION: FIRST-ORDER SYMMETRY BREAKING RESONANCES

This section demonstrates the application of local normal form techniques to a standard problem in celestial mechanics: the behavior of resonant Keplerian orbits under perturbations from a second gravitational body. While this scenario admits well-established analytical treatments in certain regimes, existing methods encounter fundamental limitations in highly perturbed cases. The local normal form approach provides a systematic framework for analyzing these challenging parameter regimes while maintaining connection to the underlying Hamiltonian structure.

The problem investigated here is the effect on first-order mean motion resonances where the perturbing body and Keplerian orbit have a $(p+1) : p$ frequency ratio. Classical Keplerian perturbation theory captures this through pendulum-like normal forms, but these approaches face a fundamental limitation – the resonant terms have strength proportional to eccentricity, so the pendulum model degenerates as $e \to 0$ when the resonant coupling vanishes. The analysis in this section circumvents these classical limitations by working directly with circular first-order resonant Keplerian orbits as the starting point, then examining how infinitesimal gravitational perturbations modify the local periodic orbit structure. At the circular resonant orbit, the Kepler degeneracy supplies an extra pair of unit multipliers in the monodromy matrix beyond the phase-energy pair, reflecting neutral motion that rotates or changes the small eccentricity vector at fixed semi-major axis. In the unperturbed limit, this subspace is center/neutral and generically diagonalizable, corresponding to the continuous family of apsidal orientations allowed by the Laplace-Runge-Lenz vector symmetry. When a perturbing secondary mass is introduced, this azimuthal symmetry breaks, and the perturbation lifts the continuous apsidal symmetry to select discrete orientations. This symmetry breaking transforms the continuous family of circular resonant orbits into discrete branches separated by π in apsidal orientation, creating the physical manifestation of the pitchfork bifurcation structure analyzed in previous sections. The local normal form approach provides a systematic method for understanding this transition while avoiding the coordinate singularities and degeneracies that plague classical

treatments.

P1-CR3BP Model

A P1-centered Planar Circular Restricted Three-body Problem (P1-PCR3BP) is constructed to isolate modifications to Keplerian orbits about P_1 while the relative mass of P_2 is increased. In contrast to the standard barycentric CR3BP formulation (BC-CR3BP), the position and mass of P_1 in the P1-CR3BP remain unchanged by the model's mass ratio parameter. Therefore, the dynamics induced by P_1 are invariant to the model's mass ratio parameter, permitting a more direct analysis of P_2's influence on deformed Keplerian orbits about P_1. For application purposes, the mass parameter between the P1-CR3BP, μ', and BC-CR3BP, μ, differ for the same physical system according to the relation:

$$\mu = \frac{\mu'}{1+\mu'} \quad \mu' = \frac{\mu}{1-\mu}$$

After deriving the P1-PCR3BP from a Lagrangian formalism, a Legendre transformation yields the Hamiltonian:

$$H(r,\theta,p_r,p_\theta) = \frac{1}{2}\left(p_r^2 + \frac{p_\theta^2}{r^2}\right) - np_\theta - \frac{1}{r} - \mu\left(\frac{1}{r_2(r,\theta)} - \frac{1}{a^2}r\cos\theta\right) \tag{2}$$

in canonical coordinates $q = [r,\theta]^\top$, $p = [p_r,p_\theta]^\top$. The two terms associated with the P2 gravitational potential result from the model frame being non-inertial with respect to P1. The equations of motion for the canonical coordinates follow Hamilton's equations $\dot{z} = \Omega\nabla_z H$, where $z = [p,q]^\top$ and Ω is the standard symplectic matrix.

Continuation Results

The numerical investigation employs two complementary continuation strategies to explore the bifurcation structure predicted by the local normal form analysis. The first setup, shown in the left panel of Figure 4, applies pseudo-arclength continuation to periodic solutions starting initially on either side of the mean motion resonance at $I_\Gamma = 0$ with circular initial conditions $\Sigma = 0$. From these seed points, tangent periodic solutions are computed iteratively with fixed mass ratio μ until the osculating eccentricity reaches $e = 0.1$, providing a local sampling of the phase space structure surrounding the resonant orbit.

The overlay of these solution curves reveals that the two sides of the mean motion resonance remain disconnected in this region of phase space, consistent with the symmetry-breaking mechanism predicted by the canonical perturbation theory. The qualitative nature of the solution curves strongly resembles that of an imperfect pitchfork bifurcation, exhibiting the characteristic cusp-like geometry derived in the previous section. In most parameter regimes where three solutions exist for a given I_Γ value, two solutions exhibit center-type stability (solid lines) while one displays hyperbolic instability (dashed lines), matching the expected stability pattern from the local normal form.

As the gravitational disturbance from P2 increases, e.g. 4:3, the imperfect pitchfork structure becomes more irregular and deviates from the idealized cubic relationship. This suggests that higher-order terms in the local Hamiltonian model become increasingly important as the perturbation strength grows beyond the small-parameter assumptions of the first-order theory. Despite these deviations at large perturbations, the fundamental bifurcation topology remains consistent

with the canonical perturbation framework. Overall, the fixed-μ continuation results demonstrate strong qualitative agreement with the theoretical predictions derived from local canonical perturbation theory, validating both the mathematical framework and its applicability to realistic orbital mechanics problems.

The second setup, illustrated in the right panel of Figure 4, constrains periodic orbit solutions to fixed longitudinal action values I_Γ while varying the perturbation strength μ. Each curve represents a pseudo-arclength continuation in both positive and negative μ directions from the unperturbed resonant orbit, revealing the complete bifurcation structure as a function of perturbation magnitude. The continuation results exhibit the cubic fold behavior predicted by the canonical perturbation theory model. For $I_\Gamma > 0$, three distinct solutions $\Sigma(\mu)$ exist until a critical perturbation strength is reached, beyond which only a single branch survives—positive Σ for positive μ and negative Σ for negative μ. At the critical values, stable and unstable periodic orbits of the same branch collide in saddle-node bifurcations, creating the fold points that bound the three-solution region.

While the cubic relationship derived from first-order canonical perturbation theory provides an excellent qualitative match, the numerical curves show some asymmetry across $\Sigma = 0$ that is not captured by the idealized model. This asymmetry likely reflects higher-order terms and nonlinear corrections that become important at finite perturbation strengths. Despite these quantitative deviations, the overall bifurcation topology demonstrates strong agreement with the locally derived perturbation theory, confirming the predictive capability of the normal form approach for understanding resonant orbital dynamics under gravitational perturbations.

REMARKS

This work demonstrates that local normal form analysis provides a systematic framework for understanding how periodic orbits in non-integrable systems respond to external perturbations. By recognizing that the tangent bundle of any periodic orbit admits locally integrable dynamics, classical Hamiltonian Perturbation Theory can be applied to predict orbit persistence and bifurcation behavior. The approach uses the monodromy matrix eigenstructure to construct canonical coordinates where perturbation effects separate into resonant and non-resonant components, enabling analysis through Lie-Deprit transformations.

The application to pitchfork bifurcations under symmetry-breaking perturbations reveals the emergence of cusp catastrophe structures, providing both qualitative insight and quantitative predictions for how periodic orbit families deform. The agreement between theoretical predictions and numerical continuation results for first-order mean motion resonances supports the approach's utility for astrodynamics applications. The methodology helps bridge the gap between analytical techniques for perturbation analysis and numerically computed nonlinear periodic orbits, offering a tool for assessing trajectory behavior in sensitive regions of phase space.

Future work could extend this framework to more complex bifurcation scenarios, including cyclic folds where the Jordan structure presents additional challenges for canonical coordinate construction. The approach's ability to predict resonant orbit behavior suggests potential applications to understanding quasi-periodic structures in ephemeris models, which may aid in trajectory design for cislunar missions. This local normal form methodology also more broadly contributes to the understanding and prediction of periodic motion persistence in non-integrable dynamical systems.

ACKNOWLEDGMENTS

A.L. thanks Beom Park, JP Almanza-Soto, Dale Williams, and Noah Sadaka for numerous insightful discussions that contributed immensely towards this research and the Multi-body Dynamics Research Group for their consistent feedback. A.L. acknowledges funding from the Fanie and John Hertz Foundation and the National Science Foundation Graduate Research Fellowship Program under Grant No. DGE-1842166.

REFERENCES

[1] G. Gómez and J. M. Mondelo, "The dynamics around the collinear equilibrium points of the RTBP," tech. rep., 2001.

[2] B. Park and K. C. Howell, "Assessment of dynamical models for transitioning from the Circular Restricted Three-Body Problem to an ephemeris model with applications," *Celestial Mechanics and Dynamical Astronomy*, Vol. 136, 2 2024, 10.1007/s10569-023-10178-9.

[3] R. Reddy Sanaga and K. C. Howell, "Leveraging the Hill Restricted Four-Body Problem to Inves-1 tigate the Ephemeris Transition Characteristics in the Earth-2 Moon L 2 Halo Orbit Region," tech. rep., 2025.

[4] B. Park and K. C. Howell, "Characterization of Earth-Moon L2 halo analogs in an ephemeris model using the elliptic restricted three-body problem," *Advances in Space Research*, Vol. 75, 3 2025, pp. 5078–5109, 10.1016/j.asr.2025.01.009.

[5] G. M. Brown, L. T. Peterson, D. B. Henry, and D. J. Scheeres, "Structure of Periodic Orbit Families in the Hill Restricted 4-Body Problem," *SIAM Journal on Applied Dynamical Systems*, Vol. 24, No. 1, 2025, pp. 346–375, 10.1137/24M1637301.

[6] A. Deprit, "Canonical transformations depending on a small parameter," *Celestial Mechanics*, Vol. 1, 3 1969, pp. 12–30, 10.1007/BF01230629.

[7] G. Gómez and J. Mondelo, "The dynamics around the collinear equilibrium points of the RTBP," *Physica D: Nonlinear Phenomena*, Vol. 157, 10 2001, pp. 283–321, 10.1016/S0167-2789(01)00312-8.

[8] H. Goldstein, C. Poole, J. Safko, and S. R. Addison, "Classical Mechanics, 3rd ed.," *American Journal of Physics*, Vol. 70, 7 2002, pp. 782–783, 10.1119/1.1484149.

[9] V. I. Arnold, *Mathematical methods of classical mechanics*. 1978.

[10] J. M. Lee, *Introduction to Smooth Manifolds*, Vol. 218. New York, NY: Springer New York, 2012, 10.1007/978-1-4419-9982-5.

[11] L. T. Peterson, *Unifying Semi-analytical and Numerical Methods for Astrodynamics Applications*. PhD thesis, University of Colorado, Boulder, 2024.

[12] G. Floquet, "Sur les équations différentielles linéaires à coefficients périodiques," *Annales scientifiques de l'École normale supérieure*, Vol. 12, 1883, pp. 47–88, 10.24033/asens.220.

[13] K. Meyer, G. Hall, and D. Offin, *Introduction to Hamiltonian Dynamical Systems and the N-Body Problem*, Vol. 90 of *Applied Mathematical Sciences*. New York, NY: Springer New York, 2009, 10.1007/978-0-387-09724-4.

[14] D. Williams, A. Langford, and K. C. Howell, "Numerical Jordan Form Construction And Applications To Astrodynamics," *AAS/AIAA Astrodynamics Specialist Conference*, Boston, 8 2025.

[15] E. M. Zimovan-Spreen, *Trajectory Design and Targeting for Applications to the Exploration Program in Cislunar Space*. PhD thesis, Purdue University, West Lafayette, 5 2021.

[16] J. Henrard and A. Lemaitre, "A second fundamental model for resonance," *Celestial Mechanics*, Vol. 30, 6 1983, pp. 197–218, 10.1007/BF01234306.

[17] S. Tremaine, *Dynamics of Planetary Systems*. 2023.

[18] V. I. Arnold, *Catastrophe Theory*. Berlin, Heidelberg: Springer Berlin Heidelberg, 1992, 10.1007/978-3-642-58124-3.

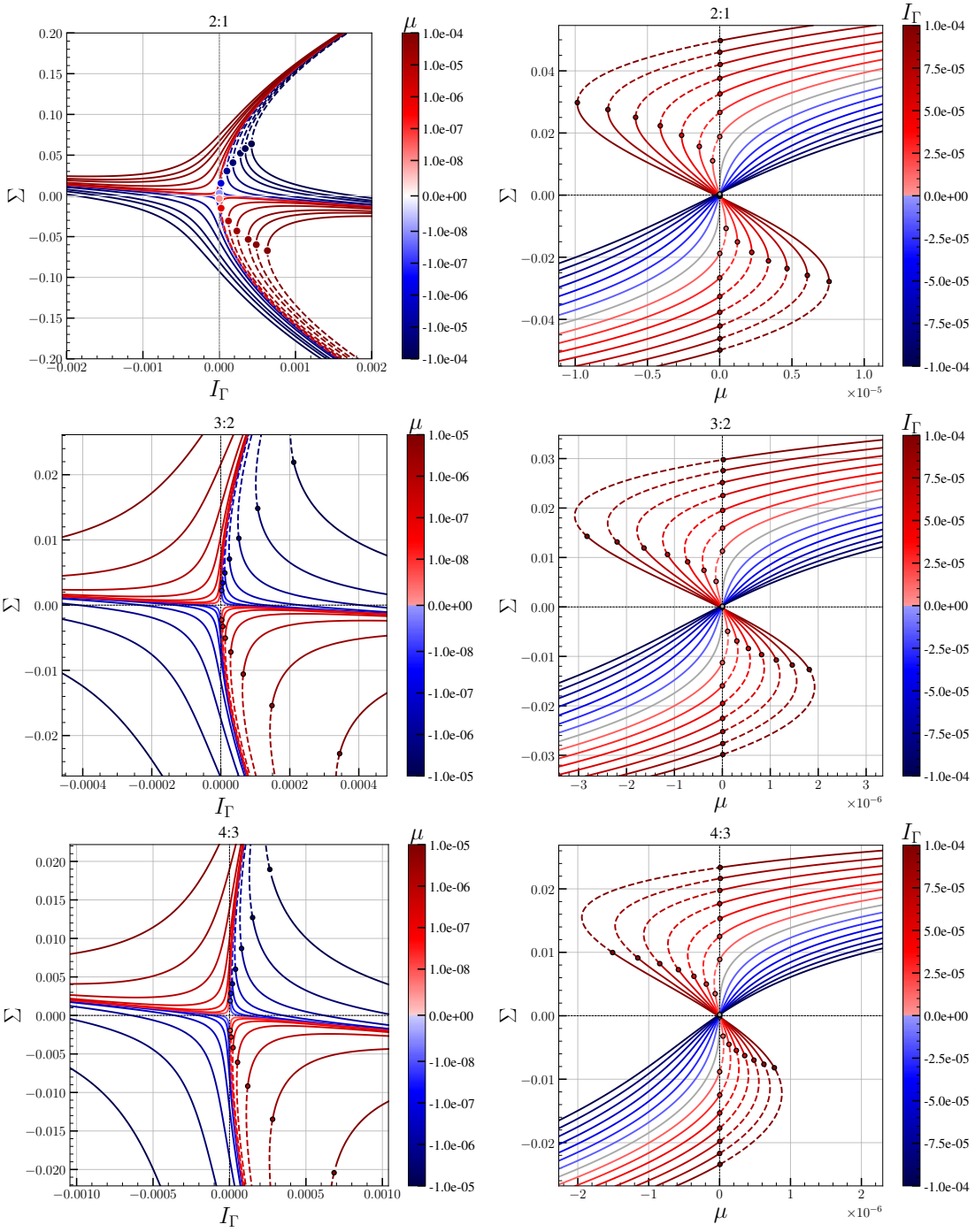

Figure 4: Numerical continuation results for periodic solutions of near-circular, interior first-order mean motion resonant orbits (2:1, 3:2, 4:3) in the P1-CR3BP. Dashed lines indicate periodic solutions with hyperbolic transverse dynamics; solid lines indicate center-type transverse dynamics. Circles approximate bifurcating solutions. **Left column:** Solution families for fixed mass ratio μ showing the relationship between longitudinal action I_Γ and signed center amplitude Σ. **Right column:** Cross-sections at fixed longitudinal action I_Γ showing how the center amplitude Σ varies with perturbation strength μ.